31st Annual International Conference of the IEEE EMBS
Minneapolis, Minnesota, USA, September 2-6, 2009

Stochastic Resonance-enhanced Laser-based Particle Detector

A. Dutta, *Member, IEEE,* and C. Werner

***Abstract*— This paper presents a Laser-based particle detector whose response was enhanced by modulating the Laser diode with a white-noise generator. A Laser sheet was generated to cast a shadow of the object on a 200 dots per inch, 512x1 pixels linear sensor array. The Laser diode was modulated with a white-noise generator to achieve stochastic resonance. The white-noise generator essentially amplified the wide-bandwidth (several hundred MHz) noise produced by a reverse-biased zener diode operating in junction-breakdown mode. The gain in the amplifier in the white-noise generator was set such that the Receiver Operating Characteristics plot provided the best discriminability. A monofiber 40 AWG (~80 μm) wire was detected with ~88% True Positive rate and ~19% False Positive rate in presence of white-noise modulation and with ~71% True Positive rate and ~15% False Positive rate in absence of white-noise modulation.**

I. Introduction

THIS paper presents a Laser-based particle detector that was used to study the Drosophila Melanogaster (fruit fly) escape behavior. The escape reaction is a behavioral trait of Drosophila Melanogaster and speciation may lead to an increased variability. The timing of the jump of a Drosophila escaping due to stimulus is of special interest since the probability of divergence would greater using a behavioral trait [1]. The detector can detect the jump and trigger a high-speed camera that can then capture the escape behavior. The particle detector is explained in details in this paper, which can be used for other particle detection applications like flow cytometry [6].

II. Methods

A. Laser-based particle detector

Figure 1 shows the arrangement where the Laser diode (Lasiris™ Mini Laser, Stocker & Yale, Inc., Canada) with the line generating optics created a uniform non-Gaussian Laser sheet. The line generating optics is a Laser line lens module that generated lines at a certain focus. Laser diode with optics created a Laser light sheet about 100μm thick. The Drosophila Melanogaster exited from a 3mm aperture and casts a shadow on a 512x1 linear sensor array (TSL208R, TAOS, Inc., USA). The input optical filter before linear sensor array high-pass filtered the incoming light at 650nm to reduce the ambient noise. Infra-red light of ~785nm wavelength is invisible to the Drosophila

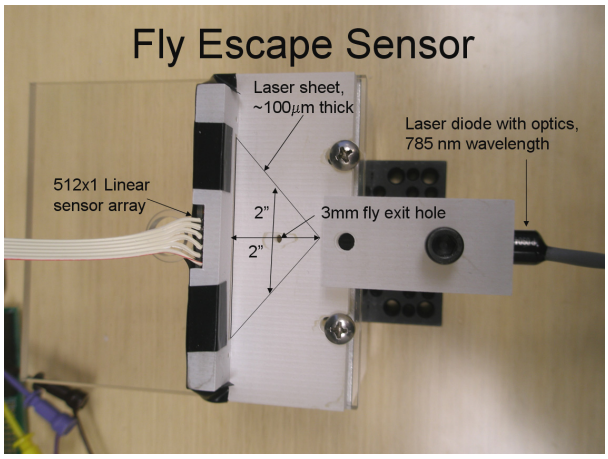

Figure 1: Fly escape detector/sensor

Melanogaster. The Laser sheet was aligned with a precisely designed and rapid prototyped holder to focus the line on a 200 dots per inch, 512x1 pixels linear sensor array. The Laser sheet was about 0.5mm above the ground surface. The pixels in the linear sensor array measure about 120μm (height) by 70μm (width). There was about 125μm center-to-center spacing and 55μm spacing between the pixels.

The 20mW, 785nm Lasiris™ Mini Laser was mounted in a rapid prototyped holder and was fixed with two set-screws such that it was facing the linear sensor array. The light energy generated an electric current in the photodiodes in the linear sensor array that was integrated for each pixel. The integration period of 1024μs was selected based on the performance of the microcontroller (20MHz external oscillator with PIC16F690, Microchip, USA) that was driving the data acquisition. The analog output from the integration circuitry for each pixel was clocked out at ~0.5MHz. The timing waveform is shown in Figure 2. The duration between the SI pulses is 1024μs and 50% duty-cycle CLK pulses were running at 0.5MHz to clock out the pixel values (AO). The pixel values or the analog output voltage is directly proportional to the light intensity and the integration period up to a saturation level of 3.5V (typically).

Manuscript received April 7, 2009.

A. Dutta and C. Werner are with the Instrument Design and Fabrication, Janelia Farm Research Campus, Howard Hughes Medical Institute, Ashburn, VA 20147 USA (e-mail: adutta@ieee.org).

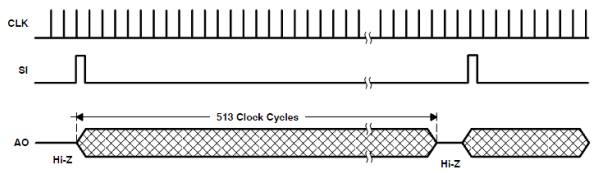

Figure 2: Timing waveform for driving TSL208R (TAOS, Inc., USA).

The drive circuitry of the Lasiris™ Mini Laser was replaced with a Laser diode constant current driver (LD1255R, ThorLabs, USA) in order to optimize the light intensity as explained in section 'Laser modulation with noise generator.' The alignment was verified by looking at the output from the linear sensor array on an oscilloscope such that all the pixels were at a uniform value.

A. Wide-bandwidth white noise generator

Figure 3 shows the white-noise generator circuit [2]. A 12V zener diode (1N759, Good-Ark, USA) was used to generate the noise when it was operated at 14V in reverse breakdown mode. The noise power from the zener diode was shown almost independent of the source power [2]. Low noise amplifiers (MAX2611, Maxim, USA) amplified

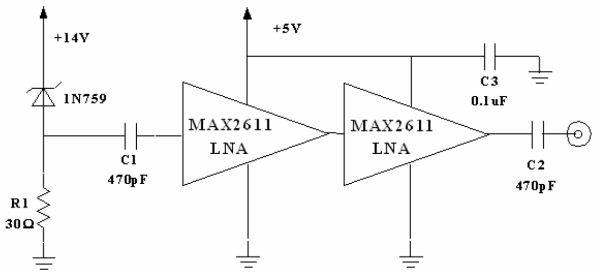

Figure 3: White-noise generator circuit (from [2]).

the noise with ~36dB gain. The amplifiers had a 3dB bandwidth from DC to 1100 MHz and a low noise figure of 3.5dB at 500 MHz. The gain of each amplifier was 18dB at 500 MHz so two amplifiers had to be cascaded to get up to ~36dB gain.

B. Laser modulation with noise generator

A Laser diode constant current driver (LD1255R, ThorLabs, USA) was used to modulate the Laser output. The operating current could be set with an external analog voltage (0–+5VDC) and a 12-turn potentiometer. The signal bandwidth was about 1.2 kHz. The 12-turn potentiometer was turned to increase the current that was observed with a digital voltmeter. The current was set such that all the pixels in the linear sensor array just reached saturation during 1024µs integration period. This drive current was close to 2mA. White-noise was added to this constant current by providing an external analog voltage to the Laser diode constant current driver from the white-noise generator circuit (Figure 3) whose amplitude was varied during the experiment.

C. Data acquisition and processing

A PICkit 2 low pin count (LPC) demonstration board (Microchip, USA) with 20-pin PIC16F690 (5 MIPS microcontroller) and a 20MHz external oscillator was used to drive the linear sensor array and acquire the pixel values. PIC16F690 has one analog comparator module (2 channels), 12 channels of 10-bit A/D, and one Enhanced Universal Synchronous Asynchronous Receiver Transmitter (EUSART) for serial communication. The EUSART in conjunction to a TTL to USB serial converter cable (TTL-232R-5V, FTDI chip, USA) was used to relay data to a virtual COM port in the PC.

PIC16F690 has 17 I/O pins. The resonator (external oscillator) was connected to pins 2 and 3. Pins 10 and 12 served as the TX and RX – EUSART lines for serial communication. Pins 4, 18, and 19 were exclusively assigned for In-Circuit Serial Programming (ICSP).

Pin 7 generated the SI pulses (Figure 2) to dictate the integration period. Pin 14 generated the CLK pulses (Figure 2) to clock out the pixel values from the linear sensor array. Pin 15 was used to read the pixel values (AO in Figure 2) from the linear sensor array. The interrupt on change was set for the comparator with each SI pulse after which the CLK pulses were generated to read the 512 pixel values from the linear sensor array with an internal voltage reference that was varied during the experiment to generate the receiver operating characteristics (ROC) plot. An interrupt caused bit 1 to be sent via EUSART to the PC at 9600 baud rate when any of the 512 pixel values was below the threshold (internal voltage reference).

During the experiment, a monofiber 40 AWG (~80 µm) wire attached to the tip of a ~3mm capillary tube was introduced manually for about 1 sec through the 3mm fly exit and then withdrawn for about 1 sec. This was repeated 20 times. When the detector detected the presence of the wire correctly then that was called True Positive. False Positive was when the detector detected the presence of wire even when there was none. The threshold value (internal voltage reference) was varied in 5 equal steps from 0 to 3.5V and the True Positive rate versus the False Positive rate was plotted for each threshold value to generate the Receiver Operating Characteristics plot. A Receiver Operating Characteristics (ROC) curve showed the tradeoff between sensitivity (i.e. True Positive rate) and 1 – specificity (i.e. False Positive rate) of the binary detector. A Discriminability Index (DI) was defined as the area under the ROC curve (AUC) which gave a measure of performance for the binary detector [3]. DI is similar to Signal-to-Noise ratio (SNR). DI was found for 5 different amplification levels that were equally spaced between 0–36dB gain for the white-noise generator.

III. RESULTS

An example of the ROC plot with and without optimum white-noise is shown in Figure 5. The monofiber 40 AWG (~80 µm) wire was detected with ~88% True Positive rate and ~19% False Positive rate in the presence of optimum white-noise modulation at threshold 2.6V. The wire was detected with ~71% True Positive rate and ~15% False Positive rate in absence of white-noise modulation at

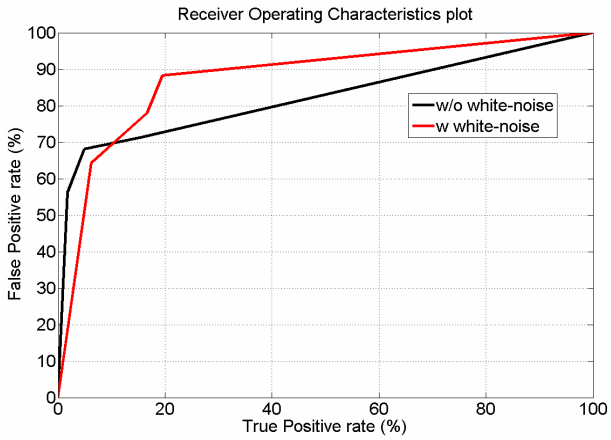

Figure 5: Receiver Operating Characteristics plot with (w: red line) and without (w/o: black line) optimum white noise levels

threshold 2.6V. The intensity of white-noise was close to optimum which enhanced the performance of the detector. The optimum amplification for the noise generator was found by looking as the change in Discrimination Index (DI) with amplification. The normalized DI (normalized by the total area of the ROC i.e., 10000) was 0.82, 0.88, 0.71, 0.63, and 0.61 for 0, 9, 18, 27, and 36 dB amplification respectively.

IV. Discussion

The improvement in the discriminability in the presence of white-noise was attributed to stochastic resonance (SR) although a more thorough analysis is necessary. The best Discriminability Index of 0.88 was obtained with 9dB amplification in the white-noise generator. Addition of noise to a bistable dynamical system (particle detector here) can improve the switching events into the two bistable states that is near-synchrony with the signal [4]. This introduces coherence into the system which can be quantified by the power spectral density of the system response. In this paper the 40 AWG wire was manually introduced and withdrawn which is currently being automated with a solenoid actuator to study more thoroughly the coherence of the system response. The light intensity from the Laser diode would be made subthreshold for the linear sensor array and the effect of increasing the intensity of white-noise on such a low contrast image would be studied to see if the DI passes through a global maximum at a critical value of the noise intensity.

The linear sensor array (TSL208R, TAOS, Inc., USA) with analog output settling time (to ±1%) equal to 185ns lends itself to a high speed imaging system with a faster microcontroller. The current work also involves particle motion estimation with Gabor filters [5]. This has applications in fluorescence based flow cytometry devices for counting microscopic particles flowing in a stream of fluid [6]. The detection rate will be enhanced with stochastic resonance while the illumination intensity would be reduced to minimize bleaching.

Acknowledgment

The fruitful discussion with Michael Reiser regarding the linear sensor array and its application to detect fly escape behavior is gratefully acknowledged.

References

[1] M. F. Snowball, and M. H. Holmqvist, “An electronic device for monitoring escape behaviour in Musca and Drosophila,” *Journal of Neuroscience Methods*, vol. 51, pp. 91-94, 1994.

[2] Link: http://pdfserv.maxim-ic.com/en/an/AN3469.pdf

[3] A. P. Bradley, "The use of the area under the ROC curve in the evaluation of machine learning algorithms," *Pattern Recognition*, vol. 30, no. 7, 1997, pp. 1145-1159.

[4] A. R. Bulsara, and L. Gammaitoni, "Tuning in to noise," *Physics Today*, vol. 49, no. 3, 1996, pp. 39-45.

[5] A. Spinei1, D. Pellerin, D. Fernandes, and J. Herault, “Fast hardware implementation of Gabor filter based motion estimation,” *Journal Integrated Computer-Aided Engineering*, vol. 7, no. 1, 2000, pp. 67-77.

[6] H. M. Shapiro, “Multistation multiparameter flow cytometry: A critical review and rationale,” *Cytometry Part A*, vol. 3, no. 4, 2005, pp. 227-243.